Journal of Alloys and Compounds, 184 (1992) 121–129
JALCOM 187

Magnetic and microstructural properties of Nd–Fe–Al alloys

R. Politano, A. C. Neiva, H. R. Rechenberg and F. P. Missell
Instituto de Física, Universidade de São Paulo, C. P. 20516, São Paulo, S. P. (Brazil)

(Received November 11, 1991)

Abstract

Arc-melted samples of Nd–(20 − x)at.%Fe–$x$at.%Al (x = 1–10) were studied by optical metallography, magnetic measurements and Mössbauer spectroscopy. The coercivity H_c and the Curie temperature T_C were determined for the as-cast samples as well as for materials annealed at 600 °C. In order to understand the annealed materials, samples with compositions Nd–58at.%Fe–5at.%Al (600 °C for 20 days) (μ phase) and Nd–47.5at.%Fe–20at.%Al (850 °C for 30 days) (δ phase) were produced and studied. It is found that annealing of arc-melted samples with x = 1–3 produces μ and other phases while, for $x > 5$, non-magnetic δ is obtained. The implications for permanent magnet production are discussed.

1. Introduction

Since the development of permanent magnets based upon the compound $Nd_2Fe_{14}B$, many attempts have been made to improve the magnetic properties by the addition of other elements. It has been found that small amounts of aluminium result in a dramatic increase in the coercivity of Nd–Fe–B magnets. Since aluminium reduces T_C and M_s slightly while leaving H_A unaltered [1], the favourable effect of the addition of aluminium to Nd–Fe–B magnets has been explained in terms of a modified microstructure [2]. Knoch *et al.* [3] found an improved wettability for aluminium-containing alloys and offered this as the explanation for the improved microstructure. The improved wetting of the grains by the neodymium-rich intergranular material results in their magnetic decoupling, thereby increasing the coercivity of the magnet.

The role of other phases found in neodymium-rich intergranular regions has also been discussed in relation to the coercivity of Nd–Fe–B magnets by Schneider *et al.* [4]. These workers found that a metastable phase with T_C = 245 °C, referred to as A_1, is formed in as-cast neodymium-rich binary and ternary alloys. The phase A_1 appears in the form of a fine eutectic microstructure which is no doubt responsible for the coercivity H_c = 4.9 kOe encountered in these materials. When the as-cast ternary alloys are annealed for short times at 600 °C, the coercivity increases to over 14 kOe because of the formation of small particles of $Nd_2Fe_{14}B$ [4, 5]. It was suggested that the dissolution of A_1 and the formation of $Nd_2Fe_{14}B$ might explain the beneficial effects of the 600 °C heat treatment in commercial magnets.

0925-8388/92/$5.00

The present work was undertaken to investigate the effect of small additions of aluminium on the magnetic properties of as-cast neodymium-rich alloys Nd–(20 − x)at.%Fe–$x$at.%Al (x = 1–10), where the magnetic properties are due mainly to A_1. It is found that T_C decreases with increasing x, and that the microstructure gradually changes from that of A_1 to a much coarser eutectic. In the annealed alloys, ferromagnetic phases are present for x = 1–3 but are absent for $x > 5$. Mössbauer spectroscopy was used to show that the μ phase (ferromagnetic) is present at low aluminium concentrations, while paramagnetic δ [6, 7] appears for the higher aluminium levels. This result suggests that the beneficial effect of aluminium in Nd–Fe–B permanent magnets may also be related to the elimination of ferromagnetic phases in the intergranular regions of annealed magnets, thereby eliminating exchange coupling between the grains.

2. Experimental details

The alloys were prepared in the form of 3–4 g buttons by arc melting under an argon atmosphere. The purities of the starting materials were 99.98% for iron, 99.9% for neodymium, and 99.999% for aluminium. Bulk samples with compositions Nd–(20 − x)at.%Fe–$x$at.%Al (x = 1, 2, 3, 5 or 10) were cut into several pieces, one of which was analysed as cast. Another was wrapped in tantalum foil and sealed in an argon-filled quartz capsule for annealing at 600 °C for 2 h. Samples with compositions Nd–47.5at.%Fe–20at.%Al and Nd–58at.%Fe–5at.%Al were also prepared by annealing for 30 days at 850 °C and for 20 days at 600 °C respectively to obtain the δ and μ phases. Energy-dispersive X-ray analysis (EDXA), as described below, showed the principal phases of these samples to have the compositions Nd–50at.%Fe–18at.%Al and Nd–62at.%Fe–6at.%Al.

All samples were examined by optical metallography using a Neophot microscope with polarized light. The Curie temperatures T_C were determined using the kink point method with a vibrating-sample magnetometer coupled to a resistive furnace. Powder diffraction patterns were obtained using Cu Kα radiation. Quantitative analyses of sample compositions using EDXA were made using a Cambridge Stereoscan 240 scanning electron microscope.

Samples for Mössbauer measurements were finely ground under dry acetone to prevent oxidation.

3. Results and discussion

3.1. As-cast samples

In Fig. 1 the Curie temperatures of the as-cast samples Nd–(20 − x)at.%Fe–$x$at.%Al are shown as a function of x for x = 1–10. We see that T_C decreases from 245 °C, a value appropriate for the A_1 phase in the binary system [4], to 162 °C for x = 10. The coercive field H_c for these

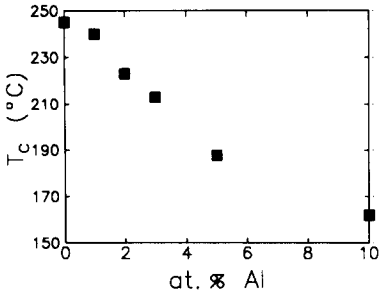

Fig. 1. Curie temperature T_C *vs.* aluminium content for as-cast samples of Nd–(20 − x)at.%Fe–$x$at.%Al.

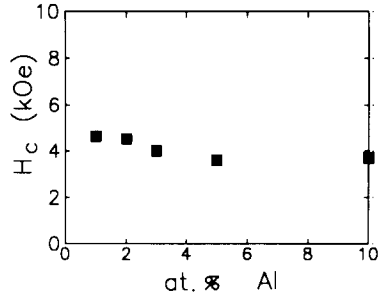

Fig. 2. Coercive field H_c *vs.* aluminium content for as-cast samples of Nd–(20 − x)at.%Fe–$x$at.%Al.

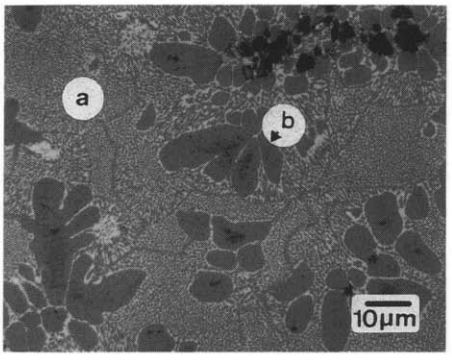

(a)

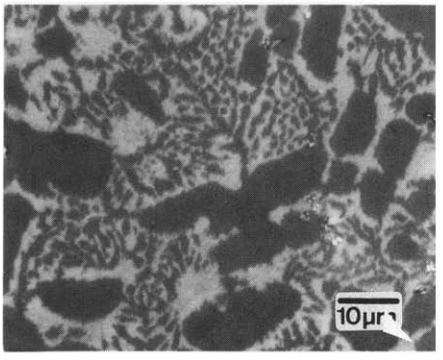

(b)

Fig. 3. Microstructures of (a) as-cast Nd–18at.%Fe–2at.%Al sharing fine fibrous A_1 + Nd eutectic a and neodymium dendrites b and (b) as-cast Nd–15at.%Fe–5at.%Al.

samples is shown in Fig. 2. We see that the coercivity is quite constant, remaining in the range 4–5 kOe for all samples. These results can be compared with those of Sanchez *et al.* [8] who studied as-cast alloys with compositions R–15at.%((1 − x)Fe–xAl) (R≡Nd, Pr; x = 0–0.7). Sanchez *et al.* [8] observed a behavior for T_C *vs.* x which is almost identical with that shown in Fig. 1. However, the coercive fields measured in ref. 8 decrease with increasing x to values slightly above 2 kOe for x = 0.7.

In Fig. 3(a) we present a micrograph of an as-cast sample of Nd–18at.%Fe–2at.%Al. The fine fibrous eutectic A_1 + Nd is very similar to that observed in binary Nd–20at.%Fe [9]. Figure 3(b) is a micrograph for as-cast Nd–15at.%Fe–5at.%Al. We see that the eutectic has coarsened considerably.

3.2. Annealed samples

It was found previously [4, 9] that annealing neodymium-rich binary Nd–Fe alloys at 600 °C resulted in the formation of the intermetallic compound Nd_5Fe_{17}, while annealing neodymium-rich ternary alloys at the same tem-

perature resulted in the formation of $Nd_2Fe_{14}B$ and another phase with $T_C = 287$ °C. Thus our Nd–Fe–Al alloys were sealed in quartz tubes for annealing at 600 °C in order to eliminate the metastable phases and to reveal those corresponding to equilibrium. Table 1 shows the values of T_C and H_c obtained for the various alloys. For the samples containing 5 and 10 at.% Al, we did not observe any Curie temperature (above room temperature) which could be associated with a ferromagnetic phase. This result is to be expected since, for these compositions Grieb *et al.* [6] found the stable phases to be Nd_3Al, neodymium and the ternary phase δ, none of which is ferromagnetic at room temperature.

As shown in Table 1, the samples with 1 and 2 at.% Al presented ferromagnetic transitions with $T_C = 250$ °C and 230 °C respectively. Annealing samples of Nd–20at.%Fe at 600 °C leads to the formation of Nd_2Fe_{17} with $T_C = 54$ °C and Nd_5Fe_{17} with $T_C = 230$ °C [9]. Thus it would be reasonable to expect the annealed samples containing small amounts of aluminium to present T_C values close to those of the binary phases. Furthermore, the stable ternary phase with the lowest aluminium content, namely μ, has presented ferromagnetic transitions in the range $T = 237$–260 °C [10]. Since we did not observe any transition at around 54 °C, it seemed improbable that Nd_2Fe_{17} had been formed. However, the Curie temperature values suggested the presence of either Nd_5Fe_{17} or μ. In Fig. 4 we show a micrograph

TABLE 1

T_C and H_c for Nd–$(20-x)$at.%Fe–$x$at.%Al samples after annealing for 2 h at 600 °C

x	T_C (°C)	H_c (kOe)
1	250	1.7
2	230	2.2
5	–	–
10	–	–

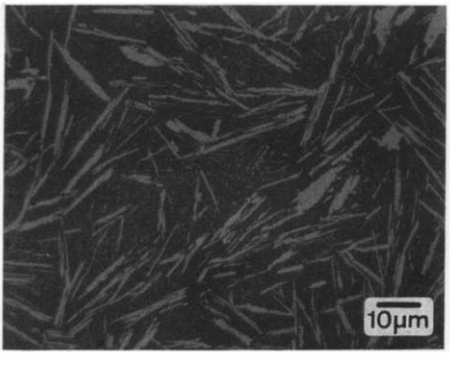

Fig. 4. Microstructure of annealed Nd–19at.%Fe–1at.%Al (600 °C for 2 h).

of the sample Nd–19at.%Fe–1at.%Al which had been annealed for 2 h at 600 °C. The fibrous eutectic of Fig. 3(a) has completely disappeared, giving rise to a microstructure similar to that encountered in annealed samples of binary Nd–Fe [9].

In order to identify the phases which had been formed in the annealed material, samples with compositions Nd–58at.%Fe–5at.%Al and Nd–47.5at.%Fe–20at.%Al were produced, as described above, to have access to the μ and δ phases respectively [6, 7]. The sample of Nd–58at.%Fe–5at.%Al was examined by X-ray diffraction and its powder pattern was found to be similar to that obtained from the μ phase [10]. The X-ray diffraction patterns are rather complex because the μ structure exhibits polytypism [11]. According to Delamare *et al.* [11], the structure consists of a long-period stacking of identical atomic layers, where each layer is shifted by a translation lattice vector with respect to the previous layer. Our sample presented a magnetization curve similar to that shown for μ in Fig. 6 of ref. 6. The Curie temperature was 240 °C and the sample presented no coercivity.

The room temperature Mössbauer spectrum of our μ sample is shown in Fig. 5. In Fig. 6 we present a Mössbauer spectrum from the sample of

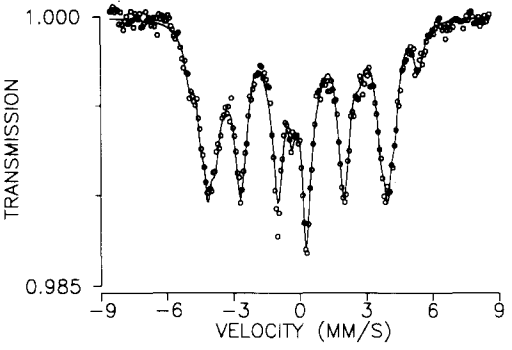

Fig. 5. Room temperature Mössbauer spectrum for Nd–58at.%Fe–5at.%Al sample annealed at 600 °C for 20 days (μ phase).

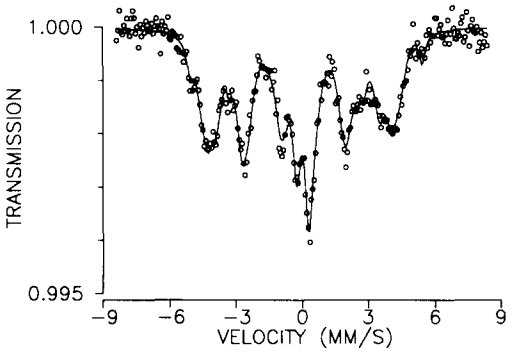

Fig. 6. Room temperature Mössbauer spectrum for Nd–18at.%Fe–2at.%Al sample annealed at 600 °C for 2 h.

Nd–18at.%Fe–2at.%Al which had been annealed at 600 °C for 2 h. Both spectra were tentatively fitted with four magnetic sextets including quadrupole interaction. In addition, it was found necessary to include a non-magnetic doublet and a gaussian hyperfine field distribution in order to account properly for the excess absorption in the central part of both spectra. The lines in each sextet were constrained to intensity ratios of $3:\alpha:1:1:\alpha:3$, with $\alpha = 2.2$–2.4 to allow for some magnetic texture. Linewidths were left free to vary independently for the five discrete subspectra. The best-fit parameters are listed in Table 2. The addition of a further sextet did not improve the fit significantly.

The hyperfine parameters of subspectra I–IV are quite similar for both samples, implying that they should correspond to the same phase (*i.e.* the μ phase). The gaussian $P(B_{hf})$ and the non-magnetic doublet, on the contrary, probably do not correspond to any definite phase, but rather to small groups of iron atoms dispersed in neodymium [12]. It must be stressed that we are not assuming the μ phase to contain just four inequivalent iron sites. Preliminary structural data [11] indeed suggest a rather complex structure for this phase. Our fitting model is intended only to provide a minimum set of parameters for a reasonable description of the Mössbauer spectrum. We note, finally, that the hyperfine parameters of subspectra I–IV are also very similar to those presented in ref. 12 for as-cast neodymium-rich binary Nd–Fe alloys. This suggests that the μ phase may be identical with one of the metastable magnetic phases referred to as A_1 and A_1' [9, 13, 14].

It is clear from the above discussion that annealing the sample with 2 at.% Al has resulted in the production of μ and that the Curie temperature measured in this sample is due to the presence of the μ phase.

X-ray diffraction of the sample of Nd–47.5at.%Fe–20at.%Al showed it to be predominantly the δ phase. EDXA measurements revealed the presence of δ and a small percentage of non-magnetic Nd_3Al, which is to be expected from the phase diagrams in refs. 6 and 7. Magnetic measurements, however,

TABLE 2

Fitted parameters from Mössbauer spectra for Nd–58at.%Fe–5at.%Al (Fig. 5) and Nd–18at.%Fe–2at.%Al (Fig. 6), where B_{hf} is hyperfine field (for the gaussian distribution, the most probable field and standard deviation (in parentheses) respectively), QS is the quadrupole splitting, and IS is the isomer shift with respect to α-Fe

Spectrum	B_{hf} (T)		QS (mm s^{-1})		IS (mm s^{-1})		Fraction (%)	
	Fig. 5	Fig. 6	Fig. 5	Fig. 6	Fig. 5	Fig. 6	Fig. 5	Fig. 6
I	32.0	32.5	0.50	0.42	0.05	0.10	13.4	5.9
II	27.0	27.5	0.25	0.01	−0.11	0.04	18.2	21.6
III	25.1	25.6	0.25	0.25	−0.10	−0.11	16.5	22.7
IV	23.1	22.8	0.26	0.11	−0.09	−0.12	33.9	29.4
Gaussian	6.3 (2.0)	5.9 (1.4)	–	–	−0.18	−0.16	14.2	7.4
Non-magnetic	–	–	0.64	0.56	0.10	0.15	3.8	13.0

revealed a Curie temperature of 180 °C associated with a residual phase, probably μ. In Fig. 7 we show the room temperature Mössbauer spectrum obtained from our sample. It is clearly non-magnetic at this temperature and any ferromagnetic phase which is present must be of the order of a few per cent. Returning now to the magnetization curve $\sigma(H)$ from this sample, we suppose that it is due to two phases: one ferromagnetic and the other paramagnetic. If we suppose the sample to contain 4% of the μ phase and subtract this contribution from the measured $\sigma(H)$ curve, then we obtain the result shown in Fig. 8. Using the measured density for this sample ($d = 6.4$ g cm^{-3}), we obtain a paramagnetic susceptibility of 2.3×10^{-4} emu g^{-1}. Returning finally to Fig. 7, we show also the Mössbauer spectrum from our annealed sample of Nd–15at.%Fe–5at.%Al. We encounter the same spectrum as that produced by our sample of δ, showing that the annealing of Nd–15at.%Fe–5at.%Al at 600 °C gave rise to δ.

The δ phase has been referred to as being antiferromagnetic [6]. Our Mössbauer measurements, however, reveal that it is not magnetically ordered at room temperature. Spectra taken at lower temperatures do exhibit magnetic

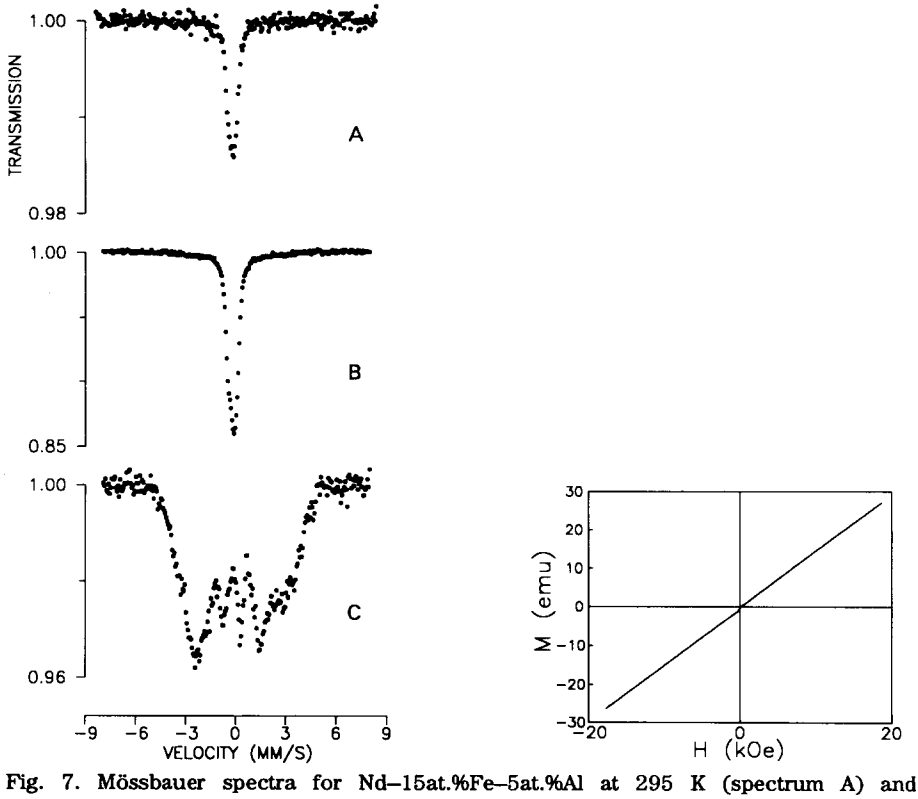

Fig. 7. Mössbauer spectra for Nd–15at.%Fe–5at.%Al at 295 K (spectrum A) and for Nd–47.5at.%Fe–20at.%Al at 295 K (spectrum B) and at 77 K (spectrum C).

Fig. 8. Specific magnetization σ *vs.* magnetic field H for Nd–47.5at.%Fe–20at.%Al (annealed at 850 °C for 30 days) after subtracting a small ferromagnetic contribution.

hyperfine splitting. In Fig. 7 we show a spectrum obtained at 77 K. It is seen to be rather complex and will be discussed in another work. We have determined the ordering temperature to be 255 ± 5 K, by measuring the Mössbauer radiation count rate at zero velocity as a function of temperature. Whether this ordering is of antiferromagnetic character is still an open question.

4. Conclusions

We have seen that 600 °C anneals of samples with low aluminium content favour the formation of ferromagnetic μ, while the presence of 5–10 at.% Al leads to the formation of the paramagnetic δ phase, in accord with the phase diagram of Grieb and coworkers [6, 7]. Without the addition of aluminium, we might expect to encounter Nd_2Fe_{17} and Nd_5Fe_{17} in the annealed samples. Knoch *et al.* [3] have suggested that the aluminium content in the intergranular regions of commercial Nd–Fe–B magnets may reach 7.5–9 at.%. If this is the case and if the effect of aluminium is similar to that which we observed in the Nd–Fe–Al alloys, then the beneficial effect of aluminium in commercial Nd–Fe–B magnets may be due in part to its role in eliminating ferromagnetic intergranular phases.

A detailed magnetic and Mössbauer characterization of the μ and δ phases is in progress.

Acknowledgments

The authors wish to acknowledge useful discussions with B. Grieb and F. J. G. Landgraf as well as the technical assistance of S. Romero and A. Santana. This work was supported by Fundação de Amparo a Pesquìsa do Estado de São Paulo, Financiadora de Estudos e Projetos and Conselho Nacional de Desenvdvimento Científico e Tecnológico.

References

1 S. Hirosawa, Y. Yamagushi, K. Tokuhara, H. Yamamoto, S. Fujimura and M. Sagawa, *IEEE Trans. Magn.*, *23* (1987) 2120.
2 K. G. Knoch, E.-Th. Henig and J. Fidler, *J. Magn. Magn. Mater.*, *83* (1990) 209–210.
3 K. G. Knoch, B. Grieb, E.-Th. Henig, H. Kronmüller and G. Petzow, *IEEE Trans. Magn.*, *26* (1990) 1951–1953.
4 G. Schneider, F. J. G. Landgraf, V. Villas-Boas and F. P. Missell, *Proc. 10th Int. Workshop on Rare Earth Magnets and Their Applications*, Vol. I, Society of Non-Traditional Technology, Tokyo, 1989, pp. 63–72.
5 V. Villas-Boas, F. P. Missell, G. Schneider, Q. Lu and D. Givord, *Solid State Commun.*, *74* (1990) 683–686.
6 B. Grieb, E.-Th. Henig, G. Martinek, H. H. Stadelmaier and G. Petzow, *IEEE Trans. Magn.*, *26* (1990) 1367–1369.

7 B. Grieb and E.-Th. Henig, *Z. Metallkd.*, *82* (1991) 560–567.
8 J. L. Sánchez, N. Suárez, S. Díaz and G. López, *J. Magn. Magn. Mater.*, (1992), in the press.
9 F. J. G. Landgraf, G. Schneider, V. Villas-Boas and F. P. Missell, *J. Less-Common Met.*, *163* (1990) 209–218.
10 B. Grieb, personal communication, 1990.
11 J. Delamare, D. Lemarchand and P. Vigier, *J. Magn. Magn. Mater.*, in the press.
12 G. C. Hadjipanayis, A. Tsoukatos, J. Strzeszewski, G. J. Long and O. A. Pringle, *J. Magn. Magn. Mater.*, *78* (1989) L1–L5.
13 F. J. G. Landgraf, F. P. Missell, H. R. Rechenberg, G. Schneider, V. Villas-Boas, J. M. Moreau, L. Paccard and J. P. Nozières, *J. Appl. Phys.*, *70* (1992) 6125–6127.
14 A. C. Neiva, T. Yonamine, F. J. G. Landgraf and F. P. Missell, *Proc. 6th Int. Symp. on Magnetic Anisotropy and Coercivity in Rare Earth–Transition Metal Alloys*, Vol. II, Carnegie–Mellon University, Pittsburgh, PA, 1990, pp. 236–249.